

Articles

Synthesis of Lamellar Mesostructures with Nonamphiphilic Mesogens as Templates

Dongyuan Zhao and Daniella Goldfarb*

Departments of Chemical Physics, The Weizmann Institute of Science, Rehovot 76100, Israel

Received November 9, 1995. Revised Manuscript Received July 15, 1996[®]

Magnesium- and zinc-based lamellar mesostructures were synthesized with nonamphiphilic mesogens as templates. The templates used were disodium chromoglycate (DSCG) and flufenamic acid (FA) which are known to exhibit lyotropic liquid-crystalline phases in aqueous solutions. Evidence for the lamellar structure was obtained from the X-ray diffraction patterns and transmission electron micrographs. The interlayer spacings in the materials prepared with DSCG and FA, 30 and 24 Å, respectively, were large compared to the molecular dimensions of the templates, suggesting the existence of a bilayer arrangement of the templates between the inorganic walls. The presence of intact template molecules within the layers was confirmed by chemical analysis, TGA, IR, and NMR measurements. Interactions between the template molecules and the inorganic layer were evident through the increase in their decomposition temperatures as compared to the pure template and by the slight weakening of the C=O bond as determined by the IR measurements. The synthesis of lamellar mesostructures with nonamphiphilic mesogens broadens the scope of the so-called "liquid-crystal template mechanism" in the sense that it is not limited to amphiphilic molecules but applies also to other molecules which can form large molecular assemblies in solutions.

Introduction

Several years ago Mobil researchers have synthesized novel silica-based mesoporous materials, termed M41S, with uniform pore sizes extending far beyond those achieved in zeolitic-like materials (15–100 Å).^{1,2} The synthesis of the M41S materials uses surfactant molecules as templates and the assembly of micellar structures of surfactants and silicate species determines the structure of the final product. The mesoporous structures obtained are MCM-41, which has a hexagonal arrangement of mesopores, MCM-50, with a lamellar structure, MCM-48, displaying a cubic structure and another phase with a cubic octamer structure.³ On the basis of the similarity of these structures to those of the lyotropic mesophases exhibited by surfactant molecules and the relation between the pore size and the length of the amphiphilic molecules, the "liquid-crystal templating" (LCT) mechanism was formulated.¹ Two possible pathways were suggested: in the first a preformed liquid-crystalline phase of the surfactant serves as a template for the formation of the solid phase,^{1,2} whereas in the second it is the cooperative organization of the silicate anions and the surfactant cations that produces

the rod like structures which then develop into the final structure of the phase.² The second pathway is in general more accepted. Evidence for the formation of a silicate–surfactant mesophase in the gel were reported from ¹⁴N NMR⁴ and ²H NMR of specifically labeled surfactants which showed spectra characteristic of partially averaged quadrupole tensors.⁵ Moreover, it has been shown that the surfactant solution itself does not necessarily possess long-range ordering and that the ordering is acquired upon the addition of the inorganic species.⁵ In this work we shall refer to the second pathway as the molecular assembly templating mechanism.

Three essential processes for the formation of the surfactant-silicate mesostructures were described:^{6,7} (i) multidentate binding of silicate oligomers, (ii) preferred polymerization of silicates at the surfactant–silicate interface, and (iii) charge density matching across the interface. Realization of the latter led to the generalization of the synthesis of periodic surfactant/inorganic composite materials.⁸ Four synthesis pathways were initially reported: the first involved the direct condensation of a cationic surfactant (S⁺) and an anionic

[®] Abstract published in *Advance ACS Abstracts*, September 15, 1996.

(1) Kresge, C. T.; Leonowicz, M. E.; Roth, W. J.; Vartuli, J. C.; Beck, J. S. *Nature* **1992**, *359*, 710.

(2) Beck, J. S.; Vartuli, J. C.; Roth, W. J.; Leonowicz, M. E.; Kresge, C. T.; Schmitt, K. D.; Chu, C. T.-W.; Olson, D. H.; Sheppard, E. W.; McCullen, S. B.; Higgins, J. B.; Schlenker, L. J. *J. Am. Chem. Soc.* **1992**, *114*, 10834.

(3) Vartuli, J. C.; Schmitt, K. D.; Kresge, C. T.; Leonowicz, M. E.; McCullen, S. B.; Hellring, S. D.; Beck, J. S.; Olson, D. H.; Sheppard, E. W. *Stud. Surf. Sci. Catal. Zeolites and related microporous materials: state of the art 1994*; Weitkamp, J., Karge, H. G., Eds.; 1994; 53.

(4) Steel, A.; Carr, S. W.; Anderson, M. W. *J. Chem. Soc., Chem. Commun.* **1994**, 1571.

(5) Firozi, A.; Kumar, D.; Bull, L. M.; Besier, T.; Sieger, P.; Huo, Q.; Walker, S. A.; Zasadzinski, J. A.; Glinka, C.; Nicol, J.; Margolese, D.; Stucky, G. D.; Chmelka, B. F. *Science* **1995**, *267*, 1138.

(6) Monnier, A.; Schuth, F.; Huo, Q.; Kumar, D.; Margolese, D.; Maxwell, R. S.; Stucky, G. D.; Krishnamurthy, M.; Petroff, P. M.; Firozi, A.; Janicke, M.; Chmelka, B. F. *Science* **1993**, *261*, 1299.

(7) Alfredsson, V.; Keung, M.; Monnier, A.; Stucky, G.; Unger, K. K.; Schuth, F. *J. Chem. Soc., Chem. Commun.* **1994**, 921.

(8) Huo, Q.; Margolese, D. I.; Ciesia, U.; Feng, P.; Gier, T. E.; Sieger, P.; Leon, R.; Petroff, P. M.; Schuth, F.; Stucky, G. D. *Nature* **1994**, *368*, 317.

inorganic species (I^-) as in the original synthesis of the M41S materials. The second pathway concerned a (S^-, I^+) pair and the third and fourth pathways employed a mediating counterion, namely, (S^+, M^-, I^+) and (S^-, M^+, I^-). Using this approach, it was possible to synthesize hexagonal, cubic, and lamellar mesostructures of oxides of antimony, tungsten, iron, lead, zinc, and others.^{8,9} This approach has been further extended to include a fifth pathway involving a neutral inorganic species, I^0 , and a neutral template, S^0 , such as primary amines¹⁰ and non-ionic poly(ethylene oxide).¹¹ Recently, gemini surfactants with two quaternary ammonium headgroups separated by a methylene chain of a variable length have been used in the synthesis of mesoporous materials.¹² Using these types of templates, in addition to the known structures MCM-41, -48, and -50 and the cubic phase with the space group $Pm\bar{3}n$,^{8,9} a new mesostructure with a three-dimensional hexagonal symmetry which does not have a liquid-crystalline analogue, have been synthesized.¹²

So far the majority of the template molecules employed in the synthesis of mesoporous materials using the molecular assembly templating mechanism, were conventional rodlike surfactant molecules with well-defined hydrophilic polar heads and long hydrophobic aliphatic chains. The lyotropic phases formed by these surfactant molecules are termed amphiphilic mesophases.¹³ There are two other classes of lyotropic mesophases, chromonic and polymeric phases.¹³ Chromonic mesophases are exhibited by molecules that usually consist of a planar aromatic moiety to which solubilizing polar groups are bonded at the periphery. Examples are disodium chromoglycate (DSCG),¹⁴ xanthone derivatives,¹⁵ and salts of flufenamic acid (FA).¹⁶ The molecular assemblies formed by these molecules are significantly different from the conventional micelles and so are the structures of their lyotropic liquid crystals.¹³ Employing such molecules as templates in the synthesis of mesoporous materials may therefore lead to new mesostructures.

In this work we report the synthesis of magnesium- and zinc-based lamellar mesostructures which were obtained with the nonamphiphilic mesogens DSCG and FA (see Figure 1). Following the principle of matching charges at the interface^{8,9} the (S^-, I^+) pathway was chosen because the templates are negatively charged.

Experimental Section

Synthesis. DSCG, often also called chromolyn, and FA were purchased from Sigma and were used without any further purification. The synthesis procedure used was similar to some of the procedures described earlier.⁹ The magnesium-based lamellar mesostructure with DSCG (LMM-C) was

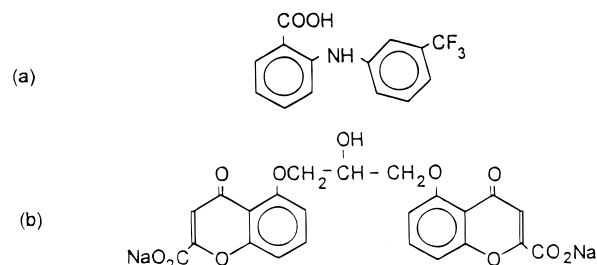


Figure 1. (a) DSCG; (b) flufenamic acid.

Table 1. Compositions (Molar Ratios) of the Synthesis Gels of the Materials Prepared and Their Final pH

material	MgO or ZnO, x	DSCG or FA, y	Na ₂ O, z	H ₂ O	pH
LMM-C	1.0	0.56–1.6	0.4–1.2	440–770	5–6
LMM-F	1.0	0.5–4.8	0.88–2.2	390–896	4–5
LMZ-C	1.0	0.5–1.25	0.4–1.0	440–890	4–5
LMZ-F	1.0	0.8–2.4	0.6–1.6	400–1000	3–4

prepared as follows: DSCG (7–20 mmol) was dissolved in water and solutions of 2 M NaOH (10–30 mmol) and 2 M Mg(NO₃)₂ (12.5 mmol) were added under stirring. The composition of the resulting gel is listed in Table 1. The gel was stirred at room temperature for 72 h and during this period a solid product appeared. The value of the final pH was 5–6. The solid was recovered by filtration, then washed with water, and dried in air at an ambient temperature. Analogous procedures were used to prepare magnesium-based lamellar materials with FA (LMM-F) and zinc-based lamellar materials with DSCG (LMZ-C) and FA (LMZ-F). In the zinc-based materials, Zn(NO₃)₂ (1 M) replaced Mg(NO₃)₂ (2 M). The composition of the gels along with the values of the final pH are listed in Table 1.

Characterization. X-ray powder diffraction measurements were carried out on a Rigaku D/Max-B X-ray diffractometer. Scanning electron micrographs were obtained using a JEOL-JSM-6400 microscope and transmission electron micrographs (TEM) were taken with a Phillips CM-12 microscope. Samples for TEM were prepared as follows: the powders to be studied were ultrasonically dispersed in distilled water and then Callodion-carbon-coated copper grids of 400 mesh were immersed in this suspension for 30 s. The grids were then dried in air at room temperature. Thermogravimetric analyses (TGA) were performed on a Mettler TA3000, and IR measurements were carried out on a Nicolet 510 FT-IR spectrometer. ¹³C solid-state NMR measurements were done at 50.5 MHz on a 200 MHz (for ¹H) home-built spectrometer. The standard CP-MAS sequence was employed with a mixing time of 2 ms, the repetition rate was 2 s, and the spinning rate was about 3 kHz. The solution spectra were recorded on a WH-270 Bruker spectrometer at 67.7 MHz.

Results

Magnesium- and Zinc-Based Lamellar Mesostructures with DSCG. Lamellar mesostructures with DSCG could be synthesized at room temperature (RT) with a relatively wide range of template/Mg molar ratios as listed in Table 1. Decreasing the ratio below this range resulted in an amorphous solid, whereas increasing it did not produce any solid. Although the typical reaction time was set to 72 h, a lamellar phase could be detected already after 5 min for both LMM-C and LMZ-C. The color of LMM-C was yellow, whereas that of LMZ-C was cream. When the synthesis was carried out at 100 °C, the product was an amorphous solid. Likewise, preparations of magnesium and zinc oxides under the same conditions without the organic templates produced amorphous solids. Increasing the amount of NaOH in the gel to $z = 2.6$ for MgO and $z =$

(9) Huo, Q.; Margolese, D. I.; Ciesla, U.; Demuth, D. G.; Feng, P.; Gier, T. E.; Sieger, P.; Firouzi, A.; Chmelka, B. F.; Schüth, F.; Stucky, G. D. *Chem. Mater.* **1994**, *6*, 1176.

(10) Tanev, P. T.; Pinnavaia, T. J. *Science* **1995**, *267*, 865.

(11) Bagshaw, S. A.; Prouzet, E.; Pinnavaia, T. J. *Science* **1995**, *269*, 1242.

(12) Huo, Q.; Leon, R.; Petroff, P. M.; Stucky, G. D. *Science* **1995**, *268*, 1324.

(13) Attwood, T. K.; Lydon, J. E.; Hall, D.; Tiddy, G. T. *Liq. Cryst.* **1990**, *7*, 657.

(14) Cox, J. S. G.; Woodard, G. D.; McCrone, W. C. *J. Pharm. Sci.* **1971**, *60*, 1458.

(15) Perahia, D.; Wachtel, E. J.; Luz, Z. *Liq. Cryst.* **1991**, *9*, 479.

(16) Kustanovich, I.; Poupko, R.; Zimmermann, H.; Luz, Z.; Labes, M. M. *J. Am. Chem. Soc.* **1985**, *107*, 3494.

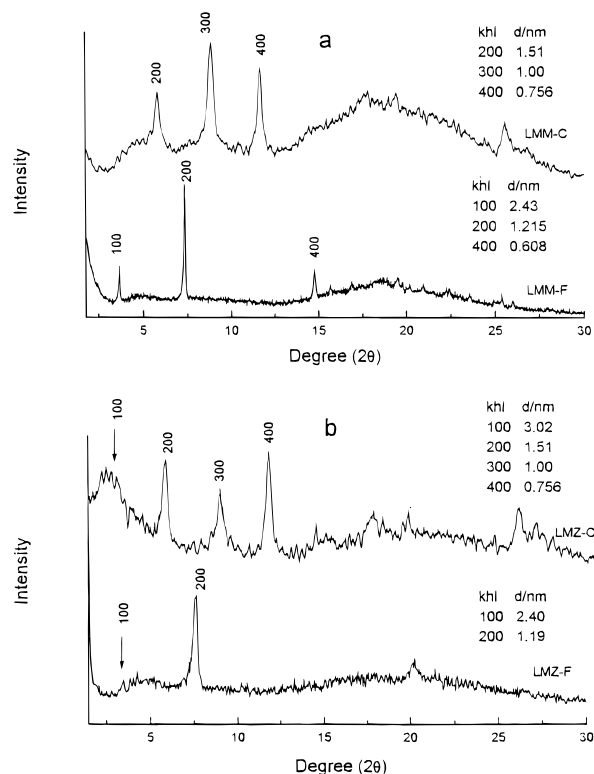
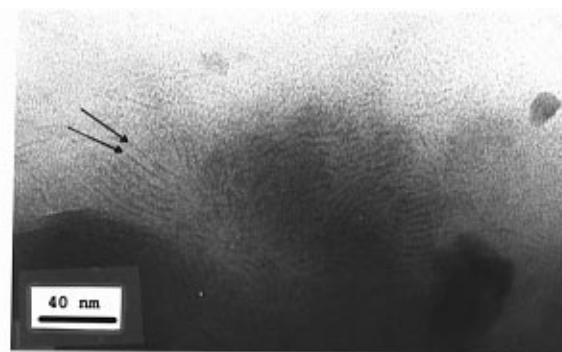


Figure 2. Powder X-ray diffraction patterns: (a) LMM-C and LMM-F; (b) LMZ-C and LMZ-F.

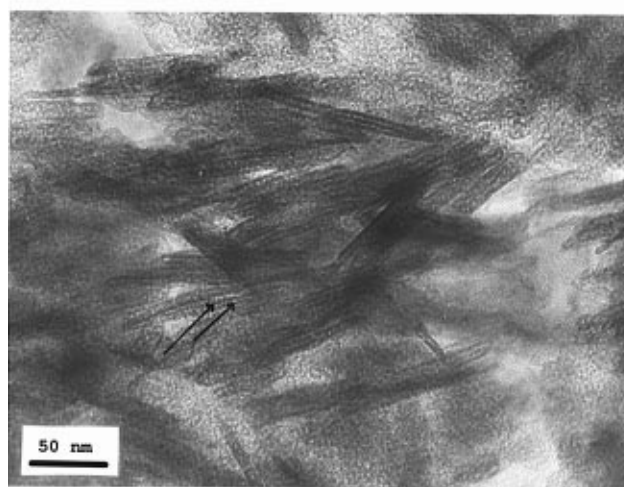
5.9 for ZnO resulted in the formation of brucite, $\text{Mg}(\text{OH})_2$ ($d_{100} = 4.78$) and zincite (hexagonal zinc oxide). Calcination of the lamellar materials and removal of the template caused the distraction of the layer structure as also observed in MCM-50.^{2,8}

Typical powder X-ray diffraction (XRD) patterns of the materials obtained with DSCG, LMM-C, and LMZ-C are shown in Figure 2. Both XRDs exhibit three major diffractions at 2θ values corresponding to d spacings of 15.1, 10.0, and 7.56 Å, which are assigned to the 200, 300, and 400 reflections. The 100 reflection is not observed in XRD of LMM-C, and in LMZ-C a broad peak appears at the position where the 100 reflection is expected. These reflections indicate a lamellar structure with an interlayer spacing of 30 Å. A few weaker reflections at higher 2θ values appear as well, the stronger one corresponding to $d \sim 3.5$ Å. The latter may be attributed to some ordering within the organic or inorganic layer. Reflections in the region of $2\theta = 20\text{--}30^\circ$ were observed also in the silicate-based lamellar phase obtained by first precipitating cubic silicate species with the cationic surfactant $\text{CH}_3(\text{CH}_2)_{15}\text{N}(\text{CH}_3)_3^+$, followed by an acidic vapor treatment.¹⁷ The layered structure of the magnesium-based materials was also evident from transmission electron micrographs of LMM-C, shown in Figure 3a. A rough estimate of the periodicity gave a value in the range 30–50 Å, which is in good agreement with the value obtained from the XRD.

Elemental analysis and TGA results obtained from LMM-C and LMZ-C, listed in Table 2, show that the materials contain relatively high levels of organics which is in agreement with the large weight loss observed in the TGA results (80–86%). For comparison



(a)



(b)

Figure 3. Transmission electron micrographs of (a) LMM-C and (b) LMM-F. The arrows point to typical layers.

Table 2. Results of Elemental Analysis and TGA of the Lamellar Materials Synthesized

sample	C/N	template/ Mg(Zn) ^{a,b} in gel	template/ Mg(Zn) in product	% wt loss (TGA)	CG/Na
LMM-C		1.2	0.78	86	1.58
LMM-F	14.7	1.0	0.28	74.9	
LMZ-C		1.25	0.88	80.9	
LMZ-F	13.9	2.4	1.42	81.2	
FA	14.0				

^a In molar ratios. ^b The relative amount of the template was calculated from the C content.

the reported weight loss of MCM-41 is ~60–65%^{9,18} and of MCM-50 is ~50%.⁹ The template/Mg ratios (0.78, 0.88) are larger than those reported for MCM-41 (0.15–0.39).¹⁹ The sample of LMM-C was also analyzed for Na^+ and the CG/Na (chromoglycate = CG) molar ratio obtained (1.58) showed that a significant amount of Na ions is present for charge balance. Considering the CG/Mg and CG/Na ratios a material with a composition of $\text{CGNa}_\alpha(\text{MgOH})_{2-\alpha}$, with $\alpha \approx 0.7$, is obtained.

The TGA curves of LMM-C, LMZ-C, and solid DSCG, shown in Figure 4, are rather similar, except for the high-temperature peak which does not appear in the lamellar materials. This suggests that the CG anions remained intact during the synthesis and that the high-

(18) Steel, A.; Carr, S. W.; Anderson, M. W. *Chem. Mater.* **1995**, *7*, 1829.

(19) Beck, J. S.; Vartuli, J. C.; Kennedy, G. J.; Kresge, C. T.; Roth, W. J.; Schramm, S. E. *Chem. Mater.* **1994**, *6*, 1861.

(17) Fyfe, C. A.; Fu, G. *J. Am. Chem. Soc.* **1995**, *117*, 9709.

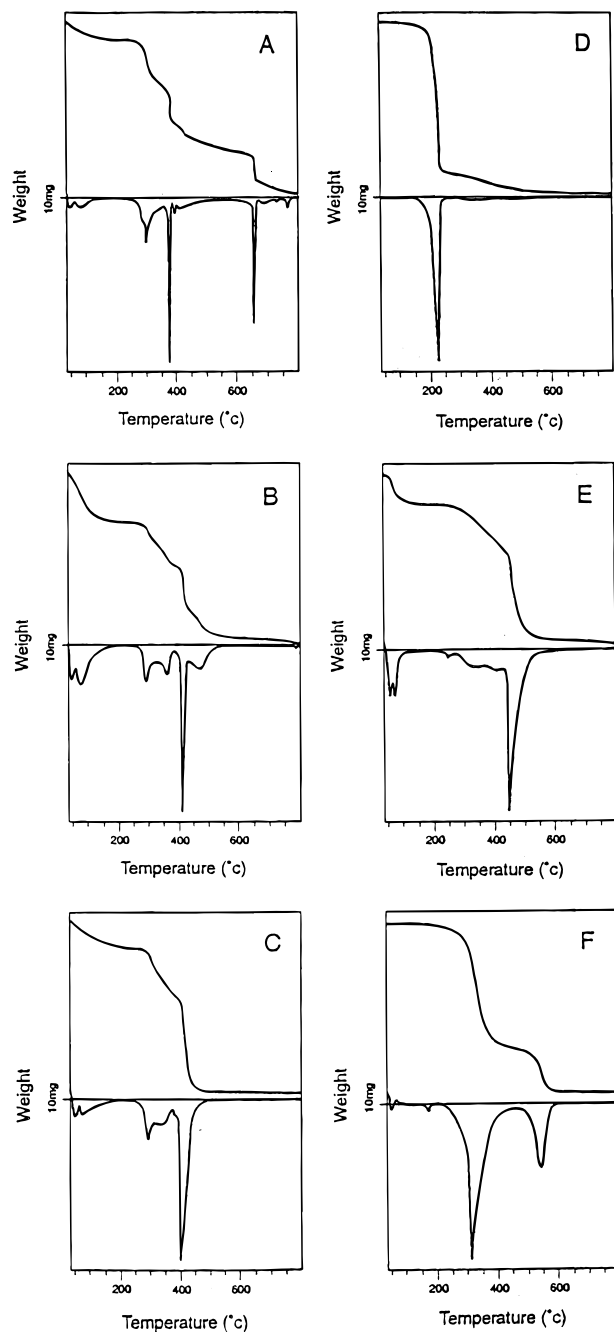


Figure 4. TGA curves of (a) DSCG, (b) LMM-C, (c) LMZ-C, (d) FA, (e) LMM-F, and (f) LMZ-F.

temperature peak in the TGA curve of pure DSCG is associated with the Na^+ cations. The first stage of weight loss at 35–150 °C is attributed to desorption of water in analogy to the M41S materials,²⁰ whereas those at 150–450 °C are due to the combustion and decomposition of the organic species.^{9,20} Within this region two features can be identified, a sharp one around 400 °C and a weaker and broader one around 300 °C. The weight loss around 400 °C is shifted toward higher temperatures in the lamellar materials as compared to the pure DSCG.

Further evidence that the organic molecules retained their molecular structure during the synthesis was obtained from ^{13}C CP-MAS NMR measurements. The

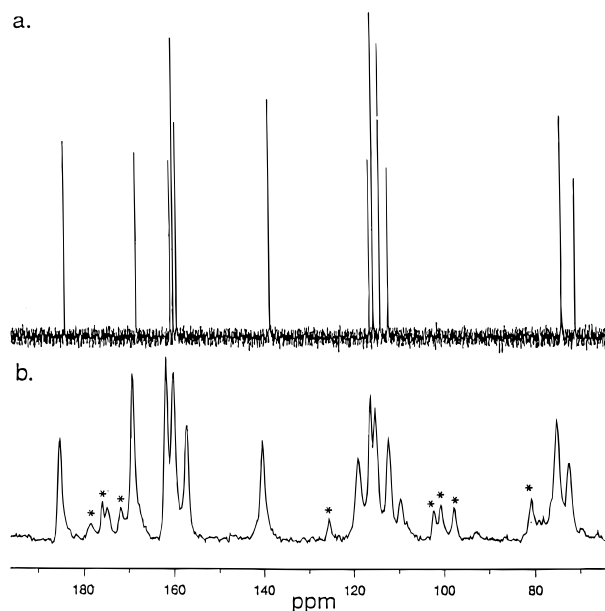
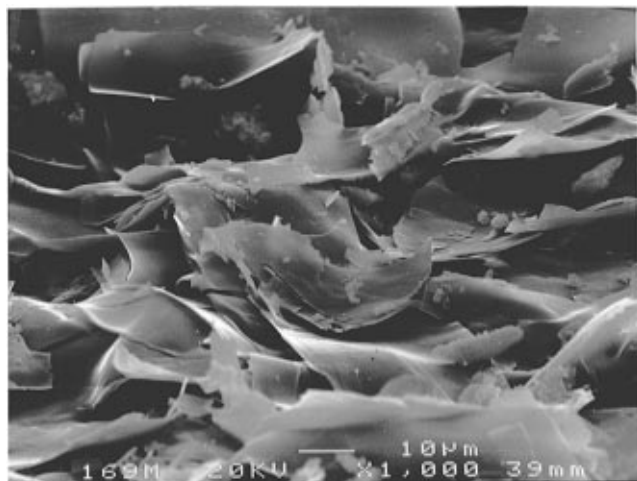


Figure 5. (a) ^{13}C NMR spectrum of a solution of DSCG in methanol. (b) ^{13}C CP MAS NMR spectrum of LMM-C. The asterisks correspond to spinning sidebands.

spectra of LMM-C and LMZ-C were similar and a comparison of the CP-MAS NMR spectrum of LMM-C with that of DSCG in a methanol solution is presented in Figure 5. Except for the broadening effects the spectra are similar. This confirms that CG anions were present in the sample. Moreover, the appearance of numerous sidebands (Figure 6b) indicates that the motion of CG anions is rather restricted. The FTIR spectra of as-synthesized LMM-C and LMZ-C were essentially identical with those of the solid DSCG, except for differences in the region 1500–1700 cm^{-1} . The carbonyl band of DSCG appeared at 1637 cm^{-1} , whereas in LMM-C and LMZ-C it was shifted to 1625 and 1630 cm^{-1} , respectively. The shifts to lower frequencies are indicative of a weakening of the C=O bond.

Magnesium- and Zinc-Based Lamellar Mesoporous Structures with FA. The range of the FA/(Mg,Zn) ratios that led to the formation of a lamellar structure was rather large (see Table 1). As in the case of the materials made with DSCG, high-temperature synthesis (100 °C) or an increase in the base content produced amorphous solids or other structures (brucite and zincite). The XRD pattern of LMM-F is presented in Figure 2b. Three sharp peaks appear in region $2\theta = 0\text{--}15^\circ$ at positions corresponding to d values of 24.3, 12.15, and 6.08 Å. These were assigned to the 100, 200, and 400 reflections which yield a periodicity of 24.3 Å. The 300 reflection, expected at 8.1 Å, is absent from the pattern. Several low-intensity diffractions appear also at higher values of 2θ , and they may indicate some order within the organic or inorganic layers. A typical TEM micrograph of LMM-F is shown in Figure 3. It shows elongated particles with a layered structure, 3–6 layers in each, with a periodicity on the order of that determined by the XRD measurements. The low number of layers observed suggests that the particles are very thin. This is confirmed by the scanning electron micrograph of LMM-F, shown in Figure 6a, which reveals a morphology of very thin flakes ($\sim 0.1\text{--}0.5 \mu\text{m}$). From the TEM and SEM micrographs it was concluded that the

(20) Chen, C. Y.; Li, H. X.; Davis, M. E. *Microporous Mater.* **1993**, 2, 17, 27.



(a)



(b)

Figure 6. Scanning electron micrographs of (a) LMM-F and (b) LMZ-F.

planes of the layers are perpendicular to the small dimension of the flakes. The XRD pattern of LMZ-F is shown in Figure 2b. It shows a strong reflection at the position of the 200 reflection in LMM-F and a weak one at the 100 position. The 400 reflection, observed in LMM-F, is however absent. From the 100 and 200 reflections a layer spacing of 24 Å was obtained. The SEM micrographs of LMZ-F, presented in Figure 6b, shows a morphology of thin flakes as well. The flakes are, however, significantly smaller than in LMM-F, which may explain their broader XRD reflections. Unfortunately we were not able to obtain TEM micrographs of LMZ-F which showed a clear layer structure.

Chemical analysis and TGA results are listed in Table 2. In both materials the C/N ratio was similar to that of FA, indicating that the FA molecule retained its structure during the synthesis. Unlike LMM-C and LMZ-C, where the template/(Mg,Zn) ratios were similar, in LMM-F and LMZ-F they were significantly different. The ratio in LMM-F is close to that of MCM-50.¹⁹ We do not understand the high ratio in LMZ-F. The TGA curves of the as-synthesized materials along with those of pure FA are shown in Figure 4. The materials made with FA, unlike those synthesized with DSCG, exhibit TGA curves which are significantly different from those of pure solid flufenamic

acid, shown in Figure 4b. It is interesting that the curve of LMM-F shows a high resemblance to those of LMM-C and LMZ-C. In both LMM-F and LMZ-F the major peak of weight loss appeared at significantly higher temperatures than in the pure FA (220 °C vs 310 and 440 °C, respectively).

The FTIR spectra of LMM-F and LMZ-F were essentially identical with those of FA, except for differences in the carbonyl stretching frequency, which shifted from 1658 cm^{-1} in FA to 1595 and 1609 cm^{-1} , respectively. Unfortunately, the ¹³C CP-MAS NMR spectra of both LMM-F and LMZ-F suffered from a low resolution due to the fluorine dipolar couplings which prevents a straightforward comparison with the solution spectra. The spectrum did show numerous sidebands, indicating that also in these materials the template is rather immobile.

Discussion

The experimental evidence that led to the conclusion that LMM-C, LMZ-C, and LMM-F have a lamellar structure was obtained from the XRD patterns and the TEM micrographs, whereas the presence of the organic molecules in the structure was deduced from the chemical analysis and the NMR, IR, and TGA results. The layered structure is composed of an alternating arrangement of an inorganic wall, probably MgO or ZnO, and an organic bilayer. The assignment of the LMZ-F structure to a lamellar structure is, however, ambiguous because of the lower quality XRD, the absence of the TEM data and the relatively high FA/Zn ratio. There are two issues regarding the XRD results which require further elaboration. The first is the absence of the 100 reflections in LMM-C and LMZ-C and the 300 reflection in LMM-F. The relative intensities of the reflections are different from those of the lamellar MCM-50 materials. There, the most intense peak is due to the 100 reflection and the 200 and 300 reflections, not always observed, are significantly weaker.³ When the intensities of the reflections are concerned, the electron density distribution, as projected onto the layer normal and usually referred to as the profile, has to be taken into account.²¹ The intensities of the reflections do not always decrease monotonically with k . For example the peak intensities of lipid bilayers are modulated according to the packing of the fatty acid chains in the core of the bilayer. For a bilayer profile with uniformly distributed methyl groups, the intensities of the reflections decrease along the series 100, 200, 300, etc., as expected. However, when the terminal methyl groups are localized in the center of the bilayer, the amplitudes of the reflections with odd k are stronger than those of the even ones.²² An analogous situation may occur in LMM-F, but the odd reflections are the weak peaks rather than the strong peaks. An organic layer composed of the templates used in this work is expected to have a significantly different profile than the surfactant molecules in MCM-50, thus leading to a different intensity profile of the XRD peaks.

The second point that should be addressed is the extremely narrow XRD peaks ($\Delta(2\theta) = 0.1\text{--}0.2^\circ$) of

(21) Blaurock, A. E. *Biochim. Biophys. Acta* **1982**, 650, 167.

(22) Wilkins, M. H. F.; Blaurock, A. E.; Engleman, D. M. *Nature New Biol.* **1971**, 230, 72.

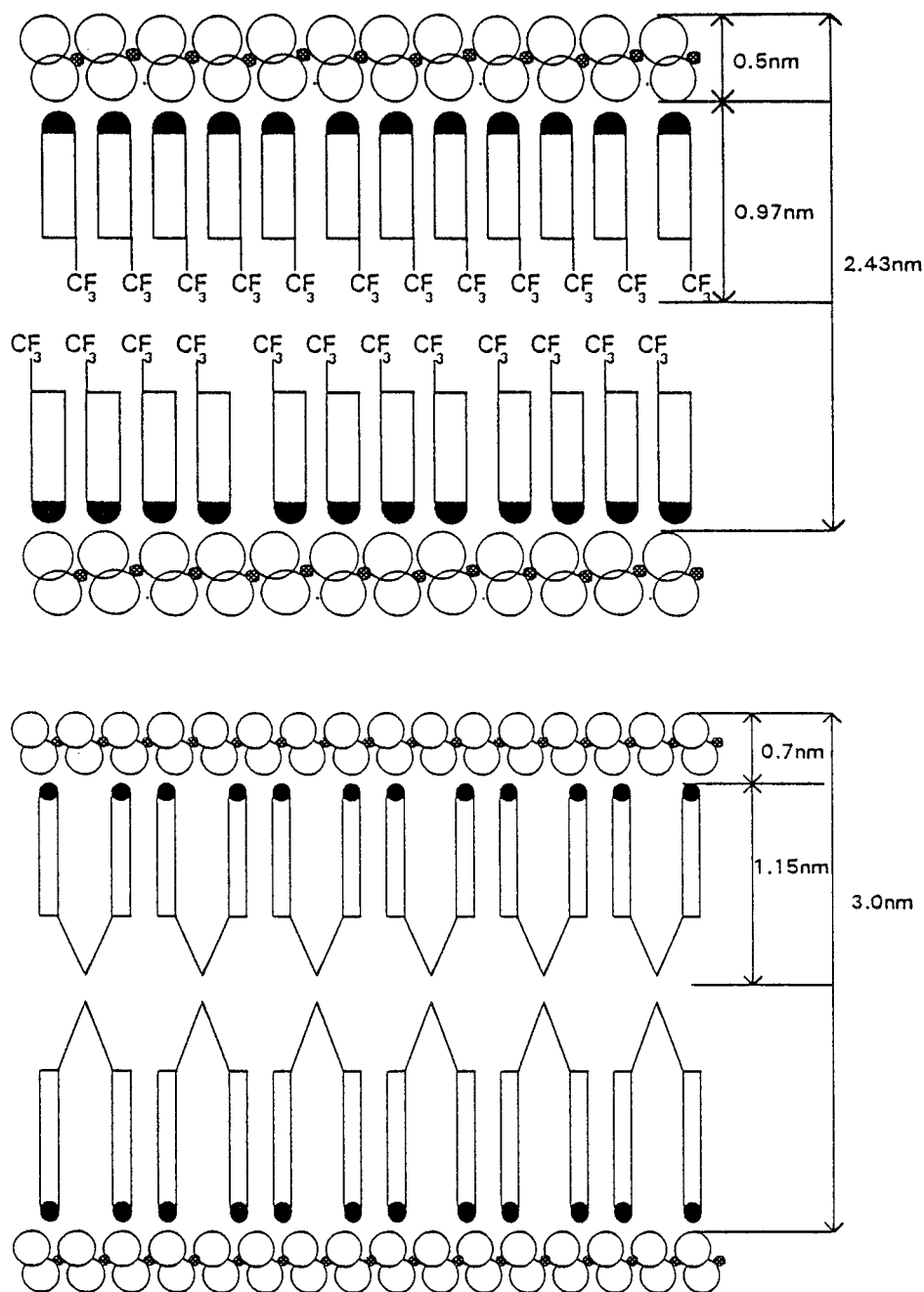


Figure 7. Schematic representation of the structure of the lamellar phases with flufenamic acid (top) and DSCG (bottom). The number of layers of atoms in the inorganic layer were arbitrarily chosen for illustrative purposes only.

LMM-F. The width of the peak can provide a lower limit to the dimension of the crystallites in the direction perpendicular to the plane of the layers, L , given by $L = \lambda / \cos \theta \Delta(2\theta)$, where λ is the X-ray wavelength.²³ For the range of $\Delta(2\theta)$ given above, the lower bound of L is estimated in the range 400–900 Å. While this is in agreement with the thickness of the LMM-F flakes shown in the SEM micrographs, it does not agree with the apparent particle thickness and the number of layers observed in the TEM micrographs. A possible explanation to this discrepancy is that the bending and folding of the edges of the thin flakes leads to a distorted picture that does not reflect the real number of layers.

The lamellar mesostructures have interlayer distances of 30 Å when synthesized with DSCG and 24 Å

when synthesized with FA. Both of these values are large compared to the size of the template molecules employed. The CG anion consists of two rigid chromone units connected via a flexible bridge, which in principle can lead to either a cis or a trans configuration. Crystal structure¹⁴ and minimum energy calculation carried out with the PC model software showed that the cis configuration is preferred and that the molecule has a length of 11.5 Å and a width of ~15 Å. The width corresponds to the distance between the edges of the two chromones (see Figure 7). Similar calculations performed on flufenamic acid resulted in a conformation where the aromatic rings are not coplanar and the molecule has a length of ~10 Å. This conformation is similar to that suggested for the molecule in the lamellar lyotropic phase.²⁴ We therefore propose a

(23) Henri, N. F. M.; Lifson, H.; Wooster, W. A. *The Interpretation of X-ray Diffraction*; McMillan & Co. Ltd.: New York, St. Martin's Press, 1961; Chapter 16.

(24) Eckert, T.; Fisher, W. *Colloid. Polym. Sci.* **1981**, 259, 553.

bilayer structure of the organic template within the organic layers for both templates as illustrated in Figure 7. In these figures the organic bilayer width was taken as twice the length of the molecule, it is also possible that one layer is shifted with respect to the other such that they can penetrate into each other, reducing the width of the organic part and increasing that of the inorganic wall. The interactions with the inorganic layer is via the carboxylate in both systems as suggested by the reduced IR frequencies of the carbonyl. The interactions, between the two layers in the organic part for LMM-C and LMZ-C involve, most probably, hydrogen bonding between the hydroxyl groups and, maybe, also water molecules. The most plausible location for the Na^+ ions is close to the carboxylates at the interface of the organic and inorganic layers.

While MCM-50 and the other lamellar phases produced from amphiphilic mesogens could be obtained also at high temperatures (100–150 °C), the materials described in this work could be synthesized only at ambient temperatures. This can be interpreted in terms of two processes that occur simultaneously during the biphasic synthesis.⁹ One is the formation of the inorganic–organic aggregates or a mesophase, which plays a key role in the organization of the inorganic material, and the second is the condensation (polymerization) of the inorganic material. If at high temperatures the mesophase or the aggregates become unstable and the second process is too fast, inorganic polymerization will occur without preorganization by the long-range ordering of the organic template. The relatively low reaction temperature with the nonamphiphilic templates may indicate either that the polymerization is faster than in the MCM-50 synthesis or that the long-range ordering of the template is stable only at lower temperatures. The phase diagrams of the flufenamic acid/water²⁴ and DSCG/water¹⁴ systems show that liquid crystalline phases are stable only up to about 60 °C, whereas the cetyltrimethylammonium bromide (CTAB)/water system exhibits lamellar and hexagonal phases at temperatures as high as 200 °C for solutions above 50% CTAB.²⁵ It is therefore plausible that this trend exists also for the corresponding inorganic–organic assemblies, suggesting that the second possibility is more likely.

Next, we discuss the possible organization of the organic–inorganic assemblies in the gel which eventually leads to the generation of the lamellar structure and their relation to the structures of the lyotropic phases of DSCG and FA. The diethylammonium salt of flufenamic acid is known to generate lamellar lyotropic phases with water.^{24,16} At low concentrations a spherical lamellar phase forms, whereas at higher concentrations a conventional planar lamellar phase is produced.^{16,24} It is therefore conceivable that initially the flufenamate anions and the Mg hydroxide (or oxide) cationic species associate to form a lamellar liquid-crystalline phase at the interface of which the oxide polymerizes, leading to the final lamellar mesostructure. The correlation with the structures of the DSCG/water liquid-crystalline mesophases is harder to envision. The mesophases formed by the DSCG/water system are the chromonic mesophases N and M.^{13,14} The N phase is a

nematic phase which consists of columns of stacked DSCG molecules with orientational order and no positional order. The N phase appears at concentrations as low as 5 wt %. In the M phase the columns are arranged in an hexagonal array.¹⁴ A third, uncharacterized phase, appearing at a low temperature (<0 °C) has been reported as well.²⁶ The aggregation of the DSCG molecules within the columns is not fully understood. It has been suggested that the columns are formed from stacked DSCG tetramers.²⁷ Thus, one might expect that the final product in the case of the DSCG template would look like a hexagonal phase rather than a lamellar phase. Although we varied the inorganic cationic species, the gel composition, the temperature, and the reaction time, we could not obtain any phase other than lamellar.

The generation of a lamellar phase and not of a columnar phase indicates that the so-called liquid crystal templating mechanism is not appropriate and it is the cooperative assembly of the organic–inorganic structures that dictates the final structure of the solid. For inorganic condensation to occur at the surface of a column one has to consider the interaction sites with the inorganic cations. In the case of a tetramer stacking within a column²⁷ there is a higher density of such sites along the column axis, but they are rather dispersed in the planes perpendicular to the columns. Therefore, it seems that polymerization along the column, leading to a final lamellar structure, will be more effective. If the asymmetric unit of the column consists of two molecules rather than four, as suggested for the chromonic phases of xanthone derivatives,¹⁵ then the formation of the lamellar phase can be envisioned as the condensation of columns due to the polymerization of the inorganic oxide. If one assumes that the third uncharacterized phase has a lamellar structure, then it is also possible that the precursor is a lamellar structure. It is interesting to note that the $\text{S}^- \text{I}^+$ pathway in the case of amphiphilic templates with phosphate or sulfonate negative headgroups and soluble cationic oxide precursors such as Mg, Al, Ga, Mn, Fe, Co, Ni, and Zn yield mainly lamellar phases as well.⁹

Finally, we rule out the possibility that the layer structure observed is just a consequence of the crystallization of the Mg/Zn salt of the cromoglycate or the flufenamate anions on the basis of the chemical analysis. The charge balance of the organic anions could be partially provided by Na^+ or H^+ ions and/or some positively charged Mg or Zn species in the inorganic wall. We also exclude the possibility that the material obtained is a double hydroxide which consist of positively charged layers separated by interlayer anions and water. The general composition of these materials is $[\text{M}_{1-x}\text{M}'_x(\text{OH})_2]^{z+} \text{X}_{z/n}^{n-} \cdot z\text{H}_2\text{O}$, where M is a monovalent or divalent cation, M' is a trivalent cation, and X is the anion which is exchangeable. The lamellar phases prepared with DSCG and flufenamic acid do not contain trivalent cations. Furthermore, the layered hydroxide synthesis usually comprises two steps, first the layered material with small inorganic anions such as nitrates is prepared and then the anions are exchanged with organic acid salts. One of the organic anions that can

(25) Auvray, X.; Petipas, R.; Anthore, R.; Roco, I.; Lattes, A. *J. Phys. Chem.* **1989**, *93*, 7458.

(26) Goldfarb, D.; Labes, M. M.; Luz, Z.; Poupko, R. *Mol. Cryst. Liq. Cryst.* **1982**, *89*, 119.

(27) Lydon, J. E. *Mol. Cryst. Liq. Cryst. Lett.* **1980**, *64*, 19.

be intercalated in the double hydroxide layer and does not give lyotropic mesophases is the benzoate anion.^{28,29} Attempts to synthesize magnesium-based lamellar materials with this anion, using the procedure described in this work, failed. We attribute the failure to the inability of the template to form organized assemblies in the gel which in turn serve as templates for the lamellar phase. We thus conclude that the driving force for the generation of the lamellar phases described in this work is the generation of large molecular assemblies, similar to those that are present in lyotropic mesophases.

Conclusions

Magnesium- and zinc-based lamellar mesostructures consisting of an inorganic wall and interlayer organic

molecules were synthesized with nonamphiphilic mesogens. The driving force for the formation of the lamellar structure was attributed to the molecular assembly templating mechanism where the templates employed, disodium chromoglycate and flufenamic acid, are known to form nonamphiphilic lyotropic liquid crystals. The synthesis of these materials broadens the scope of this mechanism to include template molecules that are not necessarily amphiphilic, yet they can self-assemble and direct the structure of the inorganic phase.

Acknowledgment. We thank Prof. S. Vega for performing the MAS NMR measurements and Dr. H. Wachtel for help with the interpretation of the X-ray data. Dr. L. Margulis, who performed the TEM measurements, passed away during the preparation of the manuscript. We dedicate this work to his memory.

CM950532S

(28) Meyn, M.; Beneke, K.; Lagaly, G. *Inorg. Chem.* **1990**, *29*, 5201.

(29) Reichle, W. T. *Chem. Tech.* **1986**, 58.

(30) Vartuli, J. C.; Schmitt, K. D.; Kresge, C. T.; Roth, W. J.; Leonowicz, M. E.; McCullen, S. B.; Hellring, S. D.; Beck, J. S.; Schlenker, J. L.; Olson, D. H.; Sheppard, E. W. *Chem. Mater.* **1994**, *6*, 2317.